



# Inhibition of soluble epoxide hydrolase alleviates insulin resistance and hypertension *via* downregulation of SGLT2 in the mouse kidney

Received for publication, December 22, 2020, and in revised form, April 7, 2021. Published, Papers in Press, April 16, 2021.

<https://doi.org/10.1016/j.jbc.2021.100667>

Jinlan Luo<sup>1,2</sup>, Shuiqing Hu<sup>2</sup>, Menglu Fu<sup>1</sup>, Liman Luo<sup>1</sup>, Yuanyuan Li<sup>1</sup> , Wenhua Li<sup>1</sup>, Yueting Cai<sup>2</sup>, Ruolan Dong<sup>3</sup>, Yan Yang<sup>4</sup>, Ling Tu<sup>1,5,\*</sup>, and Xizhen Xu<sup>2,5,\*</sup> 

From the <sup>1</sup>Department of Geriatric Medicine, <sup>2</sup>Division of Cardiology and Department of Internal Medicine, <sup>3</sup>Institute of Integrated Traditional Chinese and Western Medicine, and <sup>4</sup>Division of Endocrinology and Department of Internal Medicine, Tongji Hospital, Tongji Medical College, Huazhong University of Science and Technology, Wuhan, China; and <sup>5</sup>Hubei Key Laboratory of Genetics and Molecular Mechanisms of Cardiologic Disorders, Wuhan, China

Edited by Qi-Qun Tang

The epoxyeicosatrienoic acid (EET) exerts beneficial effects on insulin resistance and/or hypertension. EETs could be readily converted to less biological active diols by soluble epoxide hydrolase (sEH). However, whether sEH inhibition can ameliorate the comorbidities of insulin resistance and hypertension and the underlying mechanisms of this relationship are unclear. In this study, C57BL/6 mice were rendered hypertensive and insulin resistant through a high-fat and high-salt (HF-HS) diet. The sEH inhibitor, 1-trifluoromethoxyphenyl-3-(1-propionylpiperidin-4-yl) urea (TPPU), was used to treat mice (1 mg/kg/day) for 8 weeks, followed by analysis of metabolic parameters. The expression of sEH and the sodium-glucose cotransporter 2 (SGLT2) was markedly upregulated in the kidneys of mice fed an HF-HS diet. We found that TPPU administration increased kidney EET levels, improved insulin resistance, and reduced hypertension. Furthermore, TPPU treatment prevented upregulation of SGLT2 and the associated increased urine volume and the excretion of urine glucose and urine sodium. Importantly, TPPU alleviated renal inflammation. *In vitro*, human renal proximal tubule epithelial cells (HK-2 cells) were used to further investigate the underlying mechanism. We observed that 14,15-EET or sEH knockdown or inhibition prevented the upregulation of SGLT2 upon treatment with palmitic acid or NaCl by inhibiting the inhibitory kappa B kinase  $\alpha/\beta$ /NF- $\kappa$ B signaling pathway. In conclusion, sEH inhibition by TPPU alleviated insulin resistance and hypertension induced by an HF-HS diet in mice. The increased urine excretion of glucose and sodium was mediated by decreased renal SGLT2 expression because of inactivation of the inhibitory kappa B kinase  $\alpha/\beta$ /NF- $\kappa$ B-induced inflammatory response.

Diabetes mellitus (DM) manifests as a heterogeneous group of disorders characterized by hyperglycemia and glucose intolerance. Among diabetic patients, almost 50% to 70% also

suffer from hypertension, and its development coincides with the development of hyperglycemia (1–3). What is more, the prevalence of hypertension in diabetic patients is 2 to 3 times higher than that in the general population (4). Besides, hypertension is a critical factor in increasing the incidence and mortality of cardiovascular events in the course of diabetes (5). Specifically, compared with normotensive individuals with diabetes, coexisting hypertension increases the risk of cardiovascular disease and all-cause mortality by 25% and 30% (6, 7), which leads to greater health care resource use, and lower quality of life as well (1, 8). In addition, for every 10 mm Hg reduction in systolic blood pressure on average in diabetic individuals, the risk of any DM-related end point is reduced by 12%, and the risk of DM-related death is reduced by 15% (9). Therefore, it is of great significance to reduce diabetes and hypertension incidence and control blood pressure and blood glucose with reasonable drugs.

Soluble epoxide hydrolase (sEH) encoded by *EPHX2* is ubiquitously expressed in all living organisms and exists in almost all organs and tissues; it was found that the human liver possesses the highest sEH activity, followed by the kidney (10, 11). sEH functions to enzymatically hydrolyze epoxyeicosatrienoic acids (EETs) and other fatty acid epoxides (12). EETs are metabolites of arachidonic acid produced by the cytochrome P450 pathway (13). There are four regioisomers: 5,6-EET, 8,9-EET, 11,12-EET, and 14,15-EET, among them renal 14,15-EET metabolites account for up to 56.4% (14). It is reported that the sEH inhibition, an effective strategy to elevate the levels of EETs, has a therapeutic effect on multiple diseases, such as hypertension, diabetes, inflammation, stroke, dyslipidemia, immunological disorders, and so on (15). However, the effects of EETs/sEH system on diabetes accompanied by hypertension remain unknown. 1-Trifluoromethoxyphenyl-3-(1-propionylpiperidin-4-yl) urea (TPPU) is a potent inhibitor of both human and mouse sEH and selectively inhibits the hydrolase domain, thus increasing the EET levels. The pharmacokinetics of TPPU is dramatically superior to those of the 1-adamantylurea-based inhibitors, like 12-(3-adamantan-1-ylureido) dodecanoic acid. In this study, TPPU was used to

\* For correspondence: to Xizhen Xu, [xz xu@tjh.tjmu.edu.cn](mailto:xz xu@tjh.tjmu.edu.cn); Ling Tu, [lingtu@tjh.tjmu.edu.cn](mailto:lingtu@tjh.tjmu.edu.cn).

## TPPU alleviated insulin resistance and hypertension

investigate whether sEH inhibition ameliorates insulin resistance with hypertension and the potential mechanisms.

Sodium–glucose cotransporter 2 (SGLT2), encoded by the *SGLT2* family, is expressed almost exclusively in the initial convoluted portion (S1 segment) of the proximal tubule epitheliums (16, 17). SGLT2 is responsible for 97% of the body's daily glucose reabsorption, whereas SGLT1 expressed in the later parts of the proximal tubule only accounts for the remaining 3% glucose reabsorption (18). Compared with healthy individuals, there is significantly higher expression of SGLT2 in the proximal tubule in diabetics. Thus, glucose reabsorption from the glomerular filtrate is dramatically increased, leading to higher blood glucose levels (19). Recently, SGLT2 inhibitors, including dapagliflozin, empagliflozin, and canagliflozin, have been developed and widely approved in antihyperglycemic therapies. In addition to lowering blood glucose, inhibiting SGLT2 can lower blood pressure and reduce body weight (20).

In the present study, we aim to explore whether sEH inhibitor TPPU could reduce blood pressure and glucose in mice with hypertension and diabetes. Interestingly, TPPU administration ameliorated hypertension and insulin resistance by decreasing renal glucose and sodium reabsorption *via* inhibitory kappa B kinase  $\alpha/\beta$  (IKK $\alpha/\beta$ )/NF- $\kappa$ B signaling pathway-mediated SGLT2 inhibition.

### Results

#### High fat and high salt diet induced hypertension and metabolic disorder in C57BL/6 mice

At the beginning of the study, animals were fed with either a standard chow (SC)/normal salt (NS) ( $n = 24$ ) diet or a high fat and high salt (HF–HS) diet, starting with similar body weight (SC–NS =  $22.06 \pm 1.12$  g *versus* HF–HS =  $22.47 \pm 1.07$  g). After the 12-week dietary intervention, the final body weight of mice fed with an HF–HS diet was significantly higher than that of mice fed with an SC–NS diet (SC–NS =  $29.84 \pm 1.79$  g *versus* HF–HS =  $33.88 \pm 1.28$  g) (Fig. 1, A and B). Besides, these two groups showed different feeding behaviors. Specifically, the mice in HF–HS group took less food daily by 28% than that in SC–NS group, but with a higher energy intake (more than 13%) (Fig. 1, C and D), these alterations in weight gains could be attributed to the energy intake differences between the two dietary regime mice. Similarly, compared with the mice in SC–NS group, the mice in HF–HS group displayed enlarged fat depots and increased epididymal adipose tissue mass (Fig. 1, A and F). However, there was almost no difference in subscapular adipose tissue between the two groups (Fig. 1E), indicating that HF–HS diet does not affect the brown fat deposition but has obvious effects on white adipose deposition with a significantly larger adipocyte size in H&E staining (Fig. 1, A and G). Blood pressure and heart rate were evaluated at the end of the experiment. Over time, as showed in Figure 1I, there was a significant increase in systolic, diastolic, and mean blood pressure (about 30%, 23%, and 19% higher *versus* SC–NS group). However, the dietary intervention has almost no influence on heart rate (Fig. 1J). Increased fasting

blood glucose and random glucose levels were observed in HF–HS mice (Fig. 1H). Consistent with this, markedly decreased insulin sensitivity was observed in HF–HS mice compared with that in SC–NS group (Fig. 1K), and the area under the curve (AUC) of insulin tolerance in HF–HS group was about twice of that in SC–NS group (Fig. 1L). Moreover, glucose tolerance of mice in HF–HS group was suppressed significantly, resulting in an increased AUC ( $1749.83 \pm 96.12$  *versus*  $2860.00 \pm 89.50$ ) (Fig. 1, M and N). Taken together, these data indicated that an HF–HS diet resulted in increased blood pressure and insulin resistance.

#### HF–HS diet increased sEH and SGLT2 expression in the kidney

The expression of sEH and SGLT2 was evaluated by immunohistochemical (IHC) staining and Western blot (WB). The expression of sEH and SGLT2 was significantly increased in the kidney (Fig. 2, A–D). These data indicated that sEH and SGLT2 might play an important role in this animal model with insulin resistance and hypertension.

#### TPPU decreased blood pressure, improved insulin resistance, and caused a shift toward glucose utilization induced by an HF–HS diet

Our previous study demonstrated that sEH inhibitor (TPPU) inhibited SGLT2 expression to regulate glucose homeostasis in db/db mice (21). SGLT2 inhibitors as the first-line glucose-lowering medication exerted extensive cardiovascular beneficial effects. Dapagliflozin is a potent, competitive, reversible, and highly selective SGLT2 inhibitor. Compared with other SGLT2 inhibitors, dapagliflozin has higher affinity and stronger inhibitory effect on SGLT2 protein. In this study, dapagliflozin was used as a positive control. As observed, both TPPU and dapagliflozin decreased systolic blood pressure, and moreover, TPPU also decreased diastolic blood pressure and mean arterial blood pressure (Fig. 3, B–D).

As expected, TPPU treatment significantly decreased the level of fasting blood glucose as shown in Figure 3A. Moreover, TPPU administration markedly improved insulin resistance determined by glucose tolerance test and insulin tolerance test (ITT) (Fig. 3, E–H). Among these groups, dapagliflozin displayed a similar effect to TPPU in maintaining glucose homeostasis. Taken together, sEH inhibitor TPPU could exert similar effects as dapagliflozin in regulating blood pressure and blood glucose, which indicated that sEH could be a potential therapeutic target for hypertension and diabetes.

Comprehensive laboratory animal monitoring system studies was used to measure metabolic activities. There were no significant changes in the volume of oxygen consumption ( $VO_2$ ) and volume of carbon dioxide production ( $VCO_2$ ) between mice treated with an SC or an HF–HS diet, but the HF–HS diet decreased the value of respiratory exchange ratio (RER), revealed that the HF–HS diet caused a notable shift from glucose toward lipid utilization. Interestingly, administration of TPPU or dapagliflozin in an HF–HS diet-treated mice markedly increased the level of RER, which likely

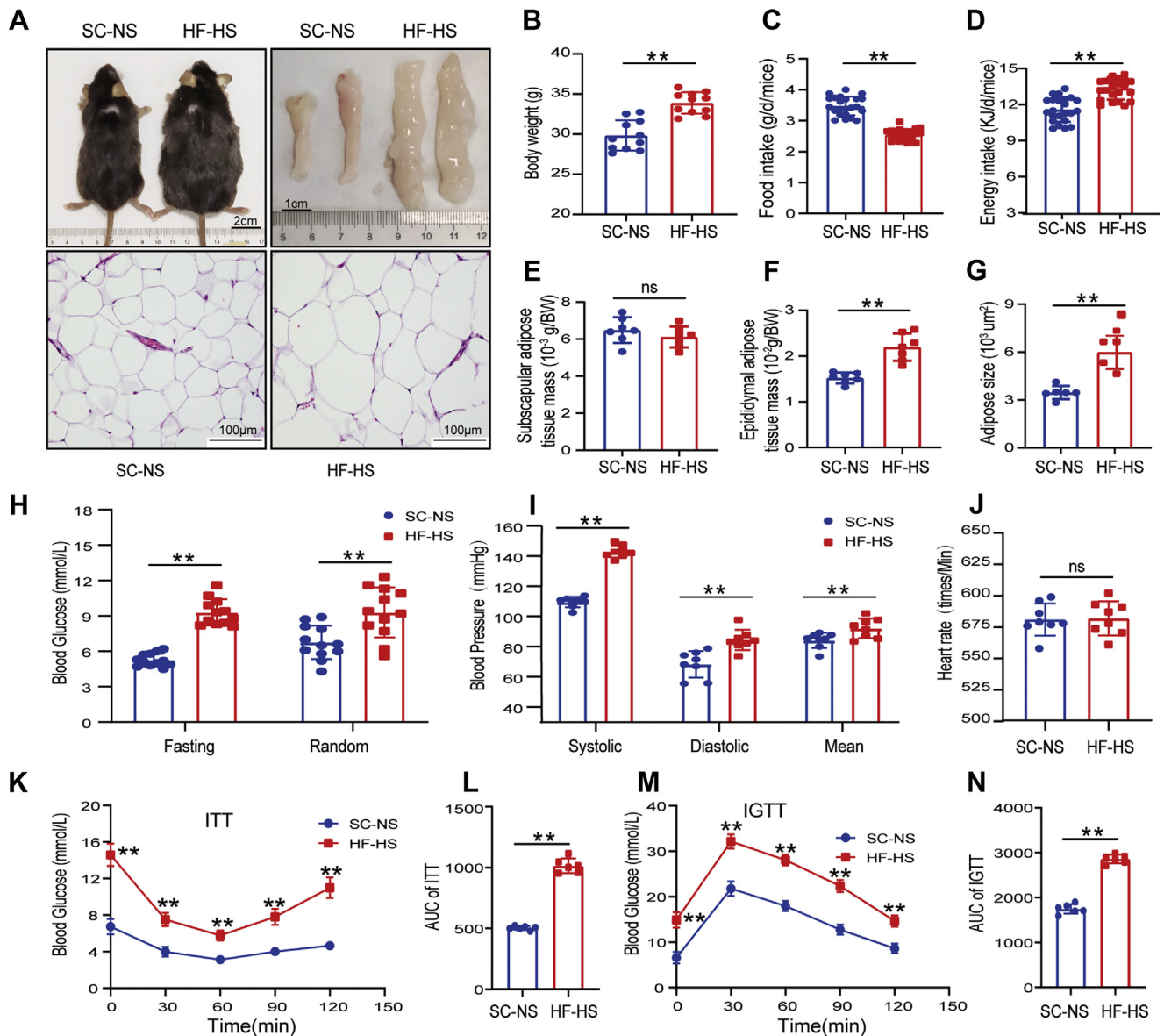


**Figure 1. High fat and high salt (HF-HS) diet induced hypertension and metabolic disorder in C57BL/6 mice.** *A*, typical examples of the mice size and adipose tissue size differences between standard chow/normal salt (SC-NS) diet and HF-HS diet after 12 weeks of treatment. Representative micrographs of epididymal adipocyte of H&E staining. *B*, changes in body weight. *C* and *D*, changes in food intake and energy intake. *E–G*, changes in subscapular and epididymal adipose tissue mass and adipocyte size of the epididymis. *H*, changes in fasting and random blood glucose. *I*, changes in systolic, diastolic, and mean blood pressures. *J*, changes in heart rate. *K* and *L*, insulin tolerance tests (ITTs) and corresponding area under the curve (AUC) analysis. *M* and *N*, intraperitoneal glucose tolerance tests (IGTTs) and corresponding AUC analysis. *n* = 6 to 12 mice in each group. Data are shown as mean ± SD. \**p* < 0.05; \*\**p* < 0.01; ns indicates *p* > 0.05.

reflected the shift from fatty acid oxidation to carbohydrate consumption (Fig. 3, *I–N*).

**TPPU administration lowered hypertension and improved insulin resistance by inhibiting sodium and glucose reabsorption mediated by 14,15-EET-triggered reduced SGLT2 expression**

To further explore the mechanisms of TPPU administration involving the regulation of blood pressure and insulin resistance, the urine volume, urine glucose, and sodium excretion among different diet and administration groups were determined. Interestingly, urine volume, urine glucose excretion,

and urine sodium excretion were markedly increased in mice treated with an HF-HS diet as shown in Figure 4, *A–C*. Importantly, TPPU treatment further increased urine volume and the excretion of glucose and sodium (Fig. 4, *A–C*). The inhibition of SGLT2 activity by dapagliflozin showed the similar effects to TPPU (Fig. 4, *A–C*).

From the IHC staining and WB results, SGLT2 expression in the kidney was significantly upregulated in mice treated with an HF-HS diet as shown in Figure 4, *D–F*. Interestingly, TPPU administration markedly prevented the upregulation in SGLT2 expression induced by an HF-HS diet treatment (Fig. 4, *D–F*). Moreover, the sEH activity in kidney was

## TPPU alleviated insulin resistance and hypertension

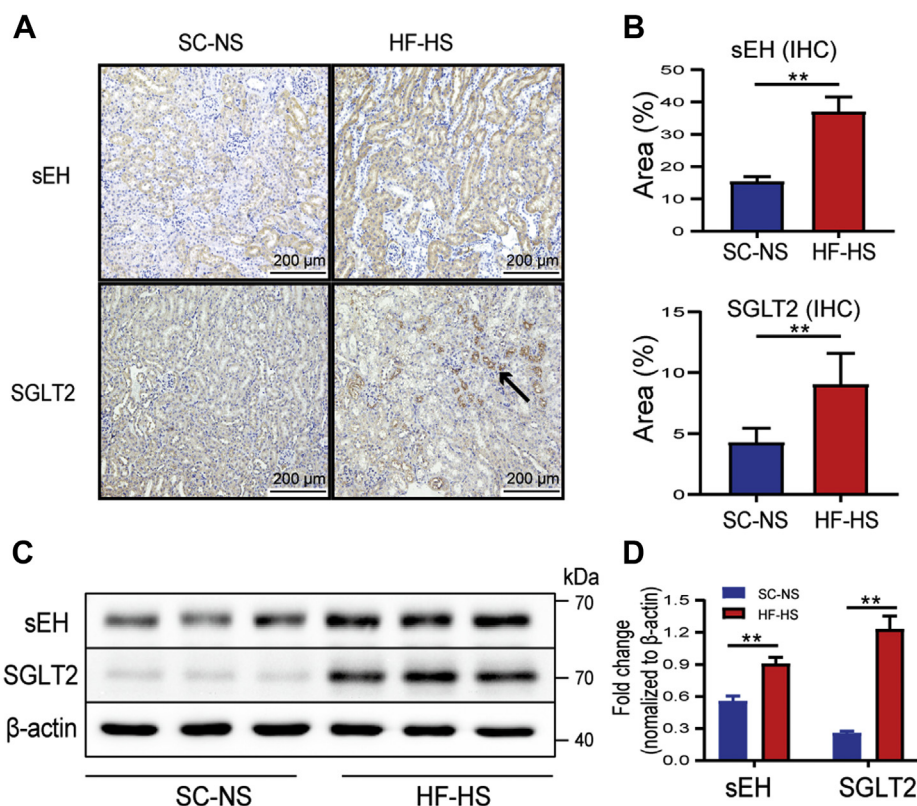


**Figure 2. HF-HS diet increased soluble epoxide hydrolase (sEH) and sodium-glucose cotransporter 2 (SGLT2) expression in the kidney.** *A*, the expression of sEH and SGLT2 in mice kidneys was evaluated by immunohistochemical staining. The *black arrow* represents the high expression area of SGLT2. The scale bar represents 200  $\mu\text{m}$ . *B*, quantitative analysis of immunohistochemical staining of sEH and SGLT2. *C* and *D*, representative Western blot and quantitation of sEH and SGLT2 expression.  $n = 6$  mice in each group. Data are shown as mean  $\pm$  SD. \*\* $p < 0.01$ . HF-HS, high-fat and high-salt; SC-NS, standard chow-normal salt.

increased, and the level of 14,15-EET in the kidney was lower in mice treated with an HF-HS diet than that in mice treated with an SC-NS diet, and moreover TPPU treatment markedly inhibited the sEH activity and thus increased the level of 14,15-EET in mice treated with an HF-HS diet, compared with that in mice without TPPU treatment as shown in Figure 4, *G* and *H*. Collectively, these data demonstrated that TPPU administration lowered hypertension and improved insulin resistance by inhibiting sodium and glucose reabsorption mediated by 14,15-EET-triggered reduced SGLT2 expression.

### TPPU treatment inhibited kidney inflammation in mice treated with an HF-HS diet

H&E staining was conducted to assess the morphological characters in the kidney. As expected, regular arrangement of renal tubular cells and glomeruli was observed in mice of the SC-NS group and SC-NS+TPPU group, and the improper arrangement of tubular cells with endocytic vacuoles was more common in the kidney of mice treated with an HF-HS diet as shown in Figure 5*A*. Importantly, TPPU treatment markedly reduced the vacuolation of the renal tubules (Fig. 5*A*).

Our previous data indicated that inflammatory response modulated the expression of SGLT2 in the kidney; so to explore whether inflammatory response was involved in this process, inflammation-related markers were determined in

this study. The level of CD68, a macrophage biomarker, was higher in the HF-HS group than that in the SC-NS group or SC-NS + TPPU group as shown in Figure 5, *A*, *B*, *F*, and *G*. Interestingly, administration of TPPU significantly inhibited the expression of CD68 induced by an HF-HS diet (Fig. 5, *A*, *B*, *F*, and *G*), which indicated that TPPU treatment markedly prevented macrophage infiltration in the kidney induced by an HF-HS diet. Furthermore, TPPU treatment markedly prevented the upregulation in interleukin-1 $\beta$  (IL-1 $\beta$ ), monocyte chemoattractant protein 1, tumor necrosis factor  $\alpha$ , and NF- $\kappa$ B expression in the kidney induced by an HF-HS diet (Fig. 5, *A*, *F*, *C-E*, and *H-J*). To further explore the anti-inflammatory mechanisms of TPPU, the IKK $\alpha$ / $\beta$ /NF- $\kappa$ B signaling pathway was detected in this study. As expected, the level of phosphor-IKK $\alpha$ / $\beta$  and phosphor-I $\kappa$ B $\alpha$  was increased, and moreover, NF- $\kappa$ B nuclear translocation was also increased in the kidney of mice treated with an HF-HS diet as shown in Figure 5, *A*, *F*, and *J*, which indicated that inflammatory response was activated by an HF-HS diet treatment. Importantly, TPPU treatment vastly decreased the level of phosphor-IKK $\alpha$ / $\beta$ , phosphor-I $\kappa$ B $\alpha$ , and NF- $\kappa$ B nuclear translocation (Fig. 5, *A*, *F*, and *J*). Taken together, these data indicated that TPPU treatment markedly inhibited kidney inflammatory response induced by an HF-HS diet treatment.

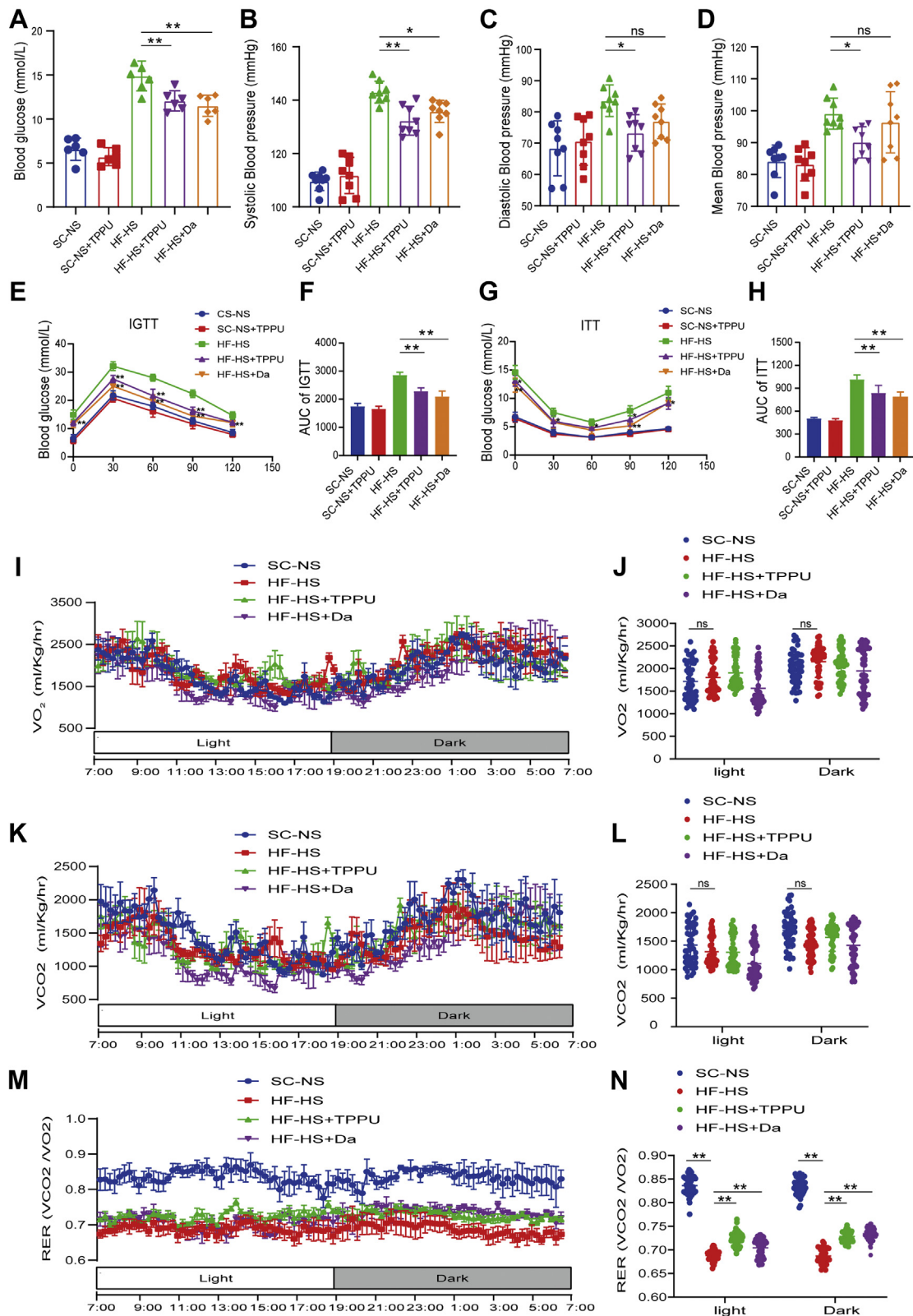


**Figure 3. Trifluoromethoxyphenyl-3-(1-propionylpiperidin-4-yl) (TPPU) decreased blood pressure, improved insulin resistance, and caused a shift toward glucose utilization induced by a high fat–high salt diet.** *A*, blood glucose after a 16-h fasting ( $n = 6$  mice). *B*, systolic blood pressure. *C*, diastolic blood pressure. *D*, mean blood pressure ( $n = 8$  mice). *E*, intraperitoneal glucose tolerance tests (IGTTs; 2 g/kg,  $n = 6$  mice). *F*, the area under the curve of IGTT. *G*, insulin tolerance tests (ITTs; 0.75 U/kg,  $n = 6$  mice). *H*, the area under the curve of ITT. *I*, dynamic changes in oxygen consumption within 24 h. *J*,  $VO_2$  (average  $O_2$  consumption normalized to body weight,  $n = 6$  mice). *K*, dynamic changes in carbon dioxide production within 24 h. *L*,  $VCO_2$  (average  $CO_2$  production normalized to body weight,  $n = 6$  mice). *M*, dynamic changes in the respiratory exchange ratio (RER;  $VCO_2/VO_2$ ). *N*, average RER =  $VCO_2/VO_2$  ( $n = 6$  mice). Data are shown as mean  $\pm$  SD. \* $p < 0.05$ ; \*\* $p < 0.01$ .

## TPPU alleviated insulin resistance and hypertension

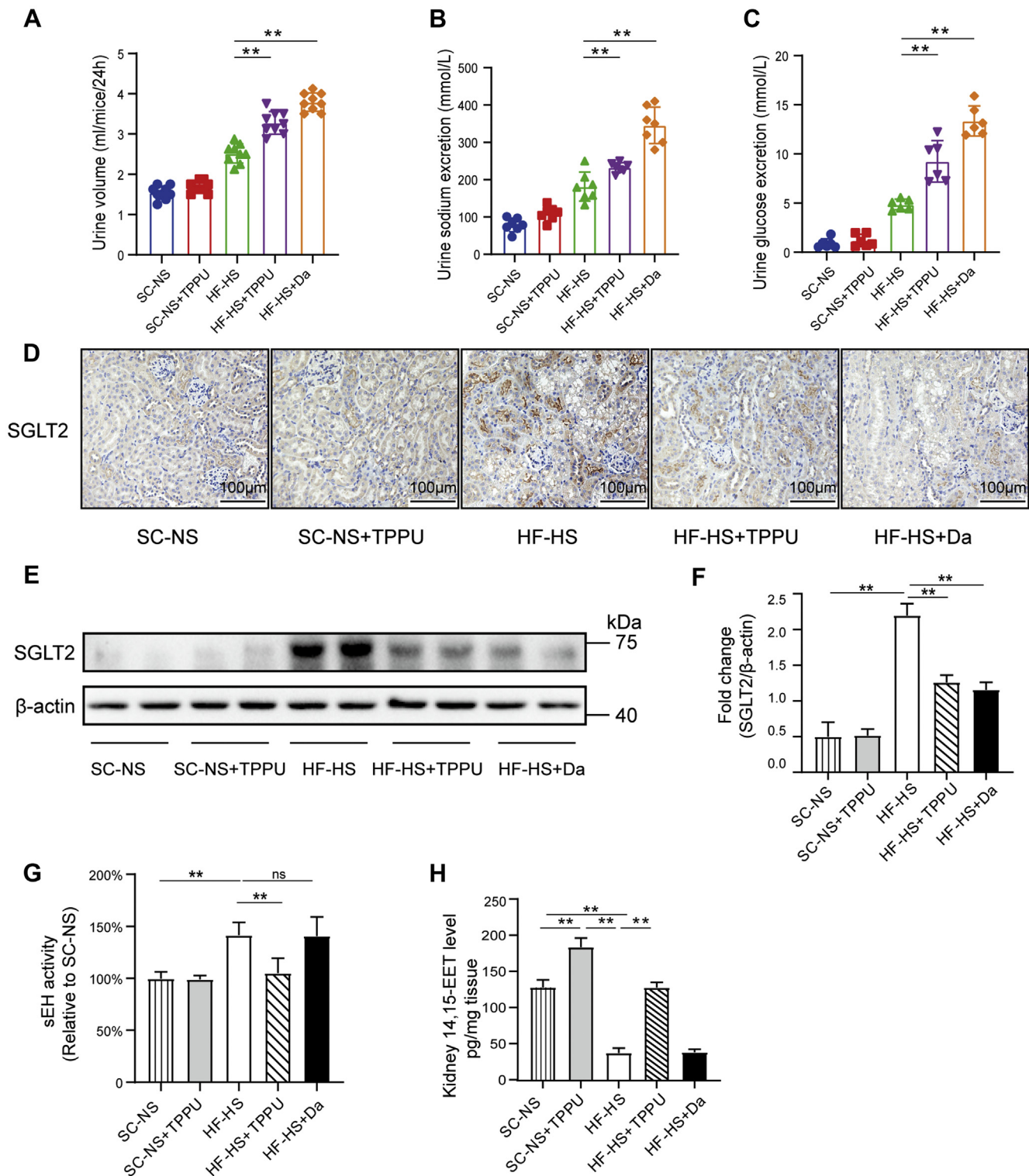


**Figure 4. TPPU administration lowered hypertension and improved insulin resistance by inhibiting sodium and glucose reabsorption mediated by 14,15-epoxyeicosatrienoic acid (14,15-EET)-triggered reduced sodium-glucose cotransporter 2 (SGLT2) expression.** *A*, urine volume ( $n = 9$  mice). *B*, urine sodium excretion ( $n = 6$  mice). *C*, urine glucose excretion ( $n = 7$  mice). *D*, representative immunohistochemical staining of SGLT2 in the kidney. The scale bar represents 100  $\mu\text{m}$ . *E* and *F*, representative Western blot and quantitation of SGLT2 in mice kidney ( $n = 6$  mice). *G*, soluble epoxide hydrolase (sEH) activity in kidney tissue ( $n = 4$  mice). *H*, 14,15-EET levels in kidney tissue ( $n = 4$  mice). Data are shown as mean  $\pm$  SD. \*\* $p < 0.01$ . EET, epoxyeicosatrienoic acid; HF-HS, high-fat and high-salt; SC-NS, standard chow/normal salt; TPPU, trifluoromethoxyphenyl-3-(1-propionylpiperidin-4-yl) urea.

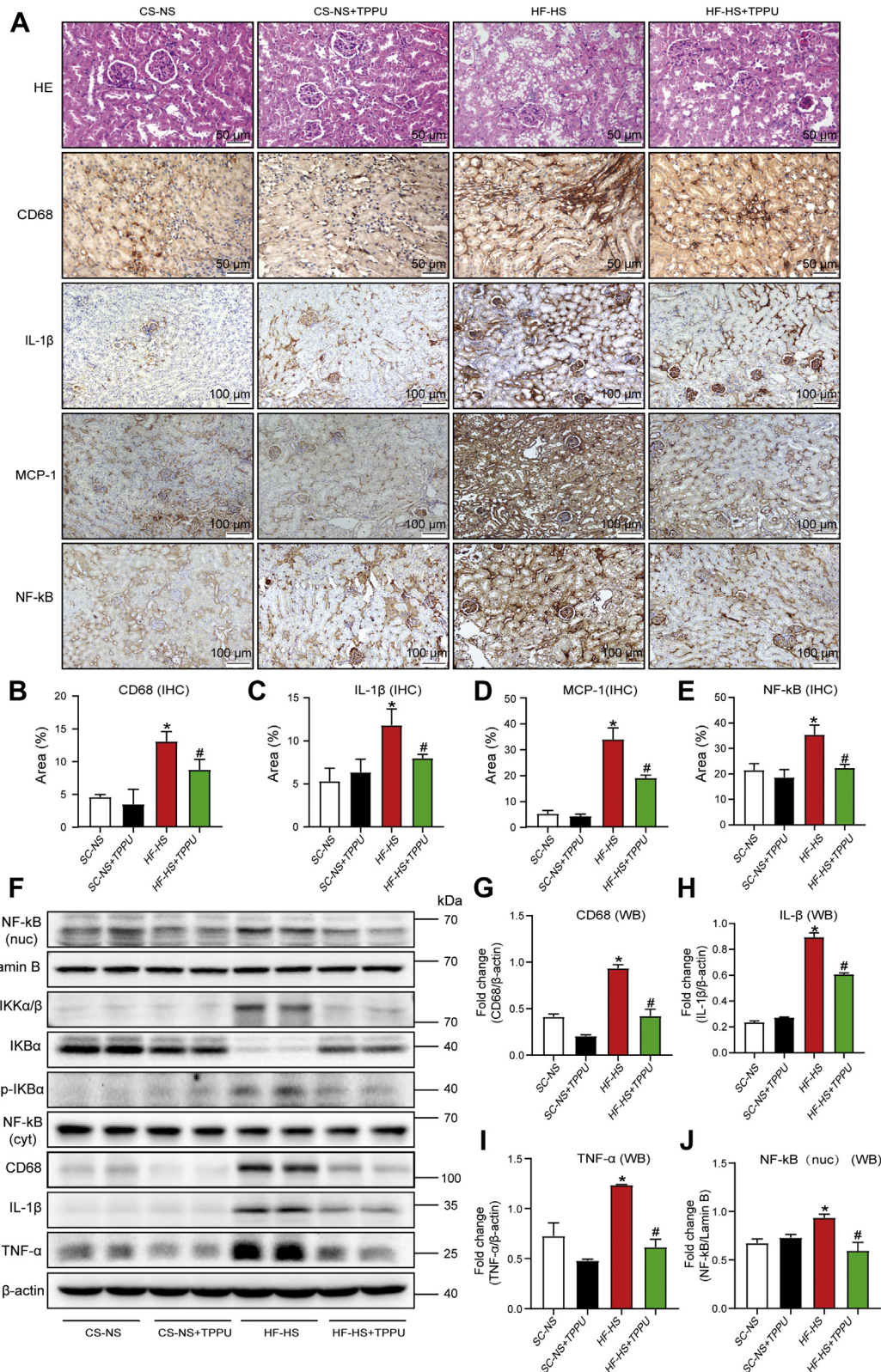


**Figure 5. Trifluoromethoxyphenyl-3-(1-propionylpiperidin-4-yl) (TPPU) treatment inhibited kidney inflammation in mice treated with a HF-HS diet.** A, representative H&E staining and immunohistochemical staining of kidney sections using anti-CD68, anti-interleukin-1β (anti-IL-1β), anti-monocyte chemoattractant protein 1 (anti-MCP-1), and anti-NF-κB antibody. B–E, quantification of CD68, IL-1β, MCP-1, and NF-κB positive area percentage. F, Western blot of phosphor-inhibitory kappa B kinase α/β (p-IKKα/β), IκBα, p-IκBα, NF-κB (nuclear and cytoplasmic), CD68, IL-1β, tumor necrosis factor α (TNF-α), and β-actin in kidney tissue. G–J, Western blot quantification of CD68, IL-1β, and TNF-α protein expression in kidney tissue normalized to β-actin, and quantification of nuclear NF-κB protein expression normalized to lamin B. n = 6 mice in each group. Data are shown as mean ± SD. \*p < 0.05 versus SC-NS group. #p < 0.05 versus HF-HS group.

## TPPU alleviated insulin resistance and hypertension

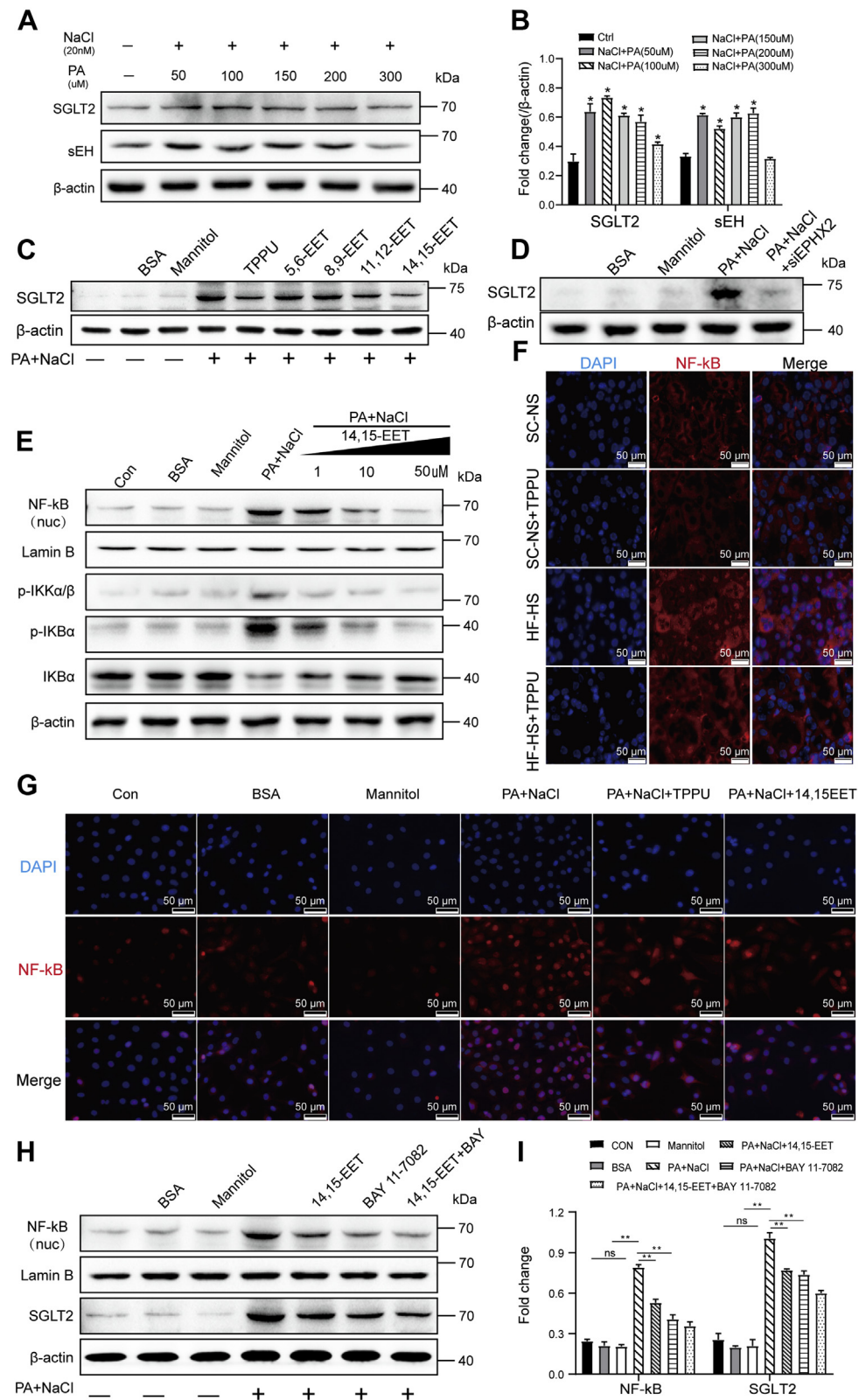


**Figure 6.** 14,15-Epoxyeicosatrienoic acid (14,15-EET) prevented the upregulation in sodium-glucose cotransporter 2 (SGLT2) expression in human proximal tubule epithelial cells (HK-2) treated with palmitic acid and NaCl via inhibiting the activation of the inhibitory kappa B kinase  $\alpha/\beta$  (IKK $\alpha/\beta$ )/NF- $\kappa$ B signaling pathway. *A* and *B*, human renal proximal tubule HK-2 cells were treated with 20 nM NaCl and different concentrations of palmitic acid, the Western blot and quantitation of SGLT2 and soluble epoxide hydrolase (sEH) expression. *C*, effects of trifluoromethoxyphenyl-3-(1-propionyl)piperidin-4-yl) urea (TPPU) and four types of EETs on NaCl and palmitic acid induced elevated SGLT2 expression in HK-2 cells. *D*, effects of siEPHX2 on NaCl and palmitic acid induced elevated SGLT2 expression in HK-2 cells. *E*, effects of different concentrations of 14,15-EET on NaCl and palmitic acid induced activation of NF- $\kappa$ B pathway, bovine serum albumin (BSA) (solvent control), and mannitol (osmotic control). *F*, representative immunofluorescence staining of NF- $\kappa$ B (red) in



### 14,15-EET prevented the upregulation in SGLT2 expression in HK-2 cells treated with palmitic acid and NaCl via inhibiting the activation of the IKK $\alpha$ / $\beta$ /NF- $\kappa$ B signaling pathway

Because SGLT2 is highly expressed in the renal tubular epithelium, human proximal tubule epithelial cells (HK-2 cells) were used to explore the regulatory mechanisms of SGLT2 expression. Dose-dependent effects of palmitic acid on SGLT2 expression were done in HK-2 cells. Interestingly, NaCl (20 nM) and palmitic acid (100  $\mu$ M) markedly increased SGLT2 and sEH expression in HK-2 cells (Fig. 6, A and B), and NaCl (20 nM) and palmitic acid (100  $\mu$ M) were used for further analysis.

Next, the effects of TPPU or EETs on SGLT2 expression in HK-2 cells treated with NaCl and palmitic acid were investigated. As expected, TPPU or EETs (11,12-EET and 14,15-EET) significantly prevented the upregulation in SGLT2 expression in HK-2 cells treated with NaCl and palmitic acid as shown in Figure 6C. Knocking down of *EPHX2* also prevented the upregulation of SGLT2 in HK-2 cells treated with NaCl and palmitic acid as shown in Figure 6D. Inflammation is a key driving factor in metabolic disorder and hypertension, and the classical IKK $\alpha$ / $\beta$ /NF- $\kappa$ B signaling pathway plays a vital role in the inflammation. As expected, phosphor-IKK $\alpha$ / $\beta$  and phosphor-I $\kappa$ B expression were increased in HK-2 cells treated with palmitic acid and NaCl. Moreover, 14,15-EET pretreatment dose dependently prevented the increase in phosphor-IKK $\alpha$ / $\beta$  and phosphor-I $\kappa$ B expression induced by palmitic acid and NaCl treatment as shown in Figure 6E.

Importantly, 14,15-EET dose dependently prevented the increase in nuclear NF- $\kappa$ B expression in HK-2 cells treated with palmitic acid and NaCl (Fig. 6E). Immunofluorescent localization of NF- $\kappa$ B further confirmed the effects of 14,15-EET on NF- $\kappa$ B translocation to the nucleus in both *in vivo* and *in vitro* studies (Fig. 6, F and G). Bovine serum albumin (BSA) (2  $\mu$ g/ml), as a solvent control for palmitic acid, and mannitol, as an osmotic control for NaCl, did not activate the IKK $\alpha$ / $\beta$ /NF- $\kappa$ B signaling pathway (Fig. 6, E and G). Interestingly, NF- $\kappa$ B inhibition by BAY 11-7082 or administration of 14,15-EET significantly prevented the increase in SGLT2 expression in HK-2 cells treated with palmitic acid and NaCl (Fig. 6, H and I). Collectively, these data revealed that 14,15-EET prevented the upregulation in SGLT2 expression in HK-2 cells treated with palmitic acid and NaCl *via* inhibiting IKK $\alpha$ / $\beta$ /NF- $\kappa$ B signaling pathway.

### Discussion

In the present study, we investigated whether TPPU treatment had a potential protective effect on insulin resistance and hypertension in mice treated with an HF–HS diet. As expected, the HF–HS diet caused obvious insulin resistance and hypertension characterized by increased body weight, blood glucose, blood pressure, and impaired glucose tolerance in

C57BL/6 mice. Interestingly, sEH and SGLT2 expression in the kidney was markedly increased in mice treated with the HF–HS diet. These data suggested that sEH and SGLT2 may be involved in this pathophysiological process. Importantly, TPPU treatment significantly improved insulin resistance and reduced hypertension with increased kidney 14,15-EET level. Moreover, TPPU administration markedly prevented the upregulation in SGLT2 expression accompanied by increased urine volume, urine glucose excretion, and urine sodium excretion, which partly accounted for the glucose-lowering and blood pressure-lowering effects of TPPU treatment. In addition, TPPU treatment markedly inhibited SGLT2 expression mediated by attenuated inflammatory response characterized by reduced macrophage infiltration and proinflammatory factor production, which was due to inactivation of IKK $\alpha$ / $\beta$ /NF- $\kappa$ B signaling pathway. Taken together, these data demonstrated that sEH inhibition alleviated insulin resistance and hypertension induced by an HF–HS diet in mice *via* increased urine glucose and sodium excretion mediated by decreased renal SGLT2 expression, which was due to inactivation of IKK $\alpha$ / $\beta$ /NF- $\kappa$ B-induced inflammatory response.

Our previous studies showed that *CYP2J3* gene delivery increased EET generation and prevented fructose-induced hypertension and insulin resistance in rats (22). Moreover, endothelium-specific *CYP2J2* overexpression in mice significantly increased 14,15-EET level, thus ameliorated age-related insulin resistance and elevated blood pressure (23). In this study, administration of TPPU also increased EET level and thus improved insulin resistance and lowered hypertension in HF–HS diet-treated mice, which was a supplement for the beneficial effects of sEH/EET system on metabolic disorders.

CYP450/EETs/sEH system has been extensively studied for its role in cardiovascular and metabolic protective effects. Cytochrome P450 epoxygenase inhibitors significantly increased mean arterial blood pressure in rats fed on an HS diet (24). *CYP2C44*<sup>(-/-)</sup> mice fed on an NS diet are normotensive but become hypertensive when fed an HS diet (25). The sEH inhibitor, 12-(3-adamantan-1-yl-ureido)-dodecanoic acid, lowered blood pressure and ameliorated renal damage in mice fed on an 8% NaCl diet for 14 days (26). Moreover, inhibition of sEH reduced blood pressure in spontaneously hypertensive rats (27). The sEH inhibitor (AR9281) decreased body weight and lowered fasting blood glucose in mice fed on a high-fat and fructose diet and diabetic db/db mice (28). The sEH inhibitor, *trans*-4-[4-(3-adamantan-1-ylureido)-cyclohexyloxy]-benzoic acid, decreased blood glucose level in mice treated with HF diet + streptozotocin/nicotinamide (29). In this study, an HF–HS diet was used to induce hypertension and insulin resistance, which was very similar to the unhealthy lifestyle in human beings. TPPU treatment improved insulin resistance and lowered hypertension in HF–HS diet-treated

kidney sections, nuclei stained with fluorescent 4',6-diamidino-2-phenylindole (DAPI) (blue). The scale bar represents 50  $\mu$ m. G, immunofluorescent localization of NF- $\kappa$ B (red) in HK-2 cells, nuclei stained with fluorescent DAPI (blue). The scale bar represents 50  $\mu$ m. H and I, effects of 14,15-EET and BAY 11-7082 (NF- $\kappa$ B inhibitor) on NaCl and palmitic acid induced elevated SGLT2 and NF- $\kappa$ B expression in HK-2 cells. Data are shown as mean  $\pm$  SD. \*\**p* < 0.01. EET, epoxyicosatrienoic acid.

## TPPU alleviated insulin resistance and hypertension

mice, which further confirmed the hypothesis that sEH deletion or inhibition had beneficial effects on the regulation of blood pressure and blood glucose in different animal models.

As a diabetic therapeutic target, SGLT2 inhibitor has been developed rapidly and attracted considerable attention for its powerful sugar-lowering effects with significant cardiovascular benefit. SGLT2 is a  $\text{Na}^+$ -D-glucose cotransporter located in the epithelial of brush-border membrane of the S1 and S2 segments of proximal renal tubules that reabsorbed sodium and glucose from crude urine in a ratio of 1:1 (30, 31). Under physiological conditions, approximately 160 to 180 g of D-glucose is filtered by the glomeruli each day and almost completely reabsorbed in the proximal tubule, SGLT2 accounts for about a proportion of 97% (32). While in diabetic individuals, SGLT2 expression and glucose uptake were increased in the proximal tubule (19), and consistent with this, multiple studies in diabetic rodent models reported increased renal SGLT2 expression as well (33). Consequently, inhibiting SGLT2 to increase glucose excretion and lower blood glucose level made it a new target of blood glucose homeostasis. In addition, the  $\text{Na}^+$ -D-glucose cotransporter is responsible for  $\text{Na}^+$  reabsorption at the same time. Thus, inhibition of SGLT2 is expected to achieve the dual effect of lowering blood glucose and blood pressure. This will provide new ideas for the treatment of patients with diabetes and hypertension.

Maintaining sodium ion homeostasis is vital for the regulation of blood pressure. The primary mechanism responsible for the blood pressure-lowering effects of CYP450 epoxigenases/EET system in salt-sensitive hypertension is increased natriuresis. For example, 14,15-EET inhibited the inward transport of sodium ions through inhibition of the epithelial sodium channel (ENaC) by an extracellular signal-regulated kinase 1/2-dependent mechanism to lower blood pressure in salt-sensitive hypertension (34). Moreover, 11,12-EET exerted an inhibitory effect on ENaC activity in rats (35). These data indicated that endogenously formed EETs or exogenously administered EETs could decrease the activity of ENaC (36). In the present study, TPPU administration markedly prevented the upregulation in SGLT2 expression accompanied by increased urine volume, urine glucose excretion, and urine sodium excretion, which partly accounted for the glucose-lowering and blood pressure-lowering effects of TPPU treatment. However, since EETs are known to activate  $\text{K}^+$  channels and inhibit ENaC activity, whether 14,15-EET inhibited SGLT2 activity *via* activating  $\text{K}^+$  channels and/or inhibit ENaC activity still needs to be further explored.

The pathogenesis of both hypertension and diabetes is related to inflammation (37, 38). Many studies demonstrated that EET/sEH system could ameliorate insulin resistance and reduce hypertension through anti-inflammatory effects (39–42). Furthermore, EETs, as an anti-inflammatory agent, exerted its influence partly by inhibiting the activation of NF- $\kappa$ B-mediated signaling pathway (43, 44). In resting cells, the I $\kappa$ B molecules sequester NF- $\kappa$ B in the cytosol and prevent its nuclear localization and transcriptional activity. Once the inhibitor of IKK complex is activated, phosphor-I $\kappa$ B will be degraded, and then NF- $\kappa$ B translocates to the nucleus to

promote transcription of target genes (45, 46). BSA (10 mg/ml) stimulates alpha-methyl-D-glucopyranoside uptake in primary rabbit renal proximal tubule cell, which is partially mediated by NF- $\kappa$ B. In addition, IL-6 increased SGLT activity through reactive oxygen species production associated with NF- $\kappa$ B signaling pathway activation in renal proximal tubule cells (47, 48). These studies reveal that NF- $\kappa$ B has a potential regulatory effect on SGLT2 expression in renal tubular epithelial cells. In this study, TPPU treatment markedly inhibited SGLT2 expression mediated by attenuated inflammatory response characterized by reduced macrophage infiltration and proinflammatory factor production, which was due to inactivation of IKK $\alpha$ / $\beta$ /NF- $\kappa$ B signaling pathway.

However, there are several limitations in this study. First, this study is almost based on rodents; so the effects and mechanisms are supposed to implement further verification in models closer to human pathophysiology. Second, because of the lack of a cellular model of hypertension and insulin resistance, palmitic acid and NaCl treatment may not fully simulate the internal environment under pathological conditions. Third, there is some possibility that other molecules may also be involved in the beneficial effects of sEH inhibition on insulin resistance and hypertension in mice treated with the HF–HS diet. Therefore, further studies should be conducted to reveal the exact molecular mechanisms. Fourth, if NF- $\kappa$ B totally mediated the insulin resistance and hypertension in mice treated with the HF–HS diet, NF- $\kappa$ B inhibitor should be applied *in vivo*. However, this was not done in the present study. Further studies should be performed to confirm this point.

In summary, sEH inhibition alleviated insulin resistance and hypertension induced by an HF–HS diet in mice *via* increased urine glucose and sodium excretion mediated by decreased renal SGLT2 expression, which was due to inactivation of IKK $\alpha$ / $\beta$ /NF- $\kappa$ B-induced inflammatory response. This study provided a new insight for the treatment of insulin resistance and hypertension.

## Experimental procedures

### Reagents and antibodies

Antibodies against the following proteins were used in this study: sEH (sc-166961; dilution 1:500 for WB, 1:200 for IHC staining), SGLT2 (sc-393350; dilution 1:500 for WB, 1:200 for IHC), CD68 (SC-17832; dilution 1:1000 for WB, 1:500 for IHC), and tumor necrosis factor  $\alpha$  (sc-12744; dilution 1:500 for WB, 1:250 for IHC) were purchased from Santa Cruz. IL-1 $\beta$  (#12242S; dilution 1:1000 for WB, 1:500 for IHC), NF- $\kappa$ B (#8242S; dilution 1:1000 for WB, 1:500 for IHC, 1:500 for immunofluorescence staining), p-IKK $\alpha$ / $\beta$  (#2697T; dilution 1:1000 for WB), p-I $\kappa$ B $\alpha$  (#2859S; dilution 1:1000 for WB), and I $\kappa$ B $\alpha$  (#4814S; dilution 1:1000 for WB) were purchased from Cell Signaling Technology, monocyte chemoattractant protein 1 (A7277; dilution 1:500 for WB), lamin B (A1910; dilution 1:1000 for WB), and  $\beta$ -actin (AC026; dilution 1:20,000 for WB) were purchased from ABclonal Technology; secondary antibodies horseradish peroxidase (HRP) goat anti-rabbit IgG (H +

L) (AS014; dilution 1:10,000 for WB), and HRP goat antimouse IgG (H + L) (AS003; dilution 1:10,000 for WB) were also purchased from ABclonal Technology. TPPU (no. 11120), 5,6-EET (no. 50211), 8,9-EET (no. 50351), 11,12-EET (no. 50511), 14,15-EET (no. 50651), and Soluble Epoxide Hydrolase Inhibitor Screening Assay Kit (no. 10011671) were purchased from Cayman Chemical. 14,15-EET/dihydroxyeicosatrienoic acids ELISA Kit (catalog no.: DH2) was purchased from Detroit R&D. Dapagliflozin (S1548) was purchased from Selleck, and palmitic acid (P5585) was purchased from Sigma-Aldrich. BSA (A8850) was purchased from Solarbio. BAY 11-7082 (HY-13453) was purchased from MCE. *EPHX2* siRNA was synthesized by Ribobio. Diaminobenzidine Detection Kit (polymer) (GK600510) was purchased from Gene Tech. Sodium Assay Kit (C002-1-1) and Glucose Assay Kit (F006-1-1) were purchased from Nanjing Jiancheng Bioengineering Institute.

### Animal treatment

Sixty six-week-old male C57BL/6 mice (GemPharmatech) were fed in controlled conditions (12-h light/dark cycle,  $22 \pm 1$  °C, and  $50 \pm 10\%$  humidity), with food and water provided ad libitum. After adapting to the environment for a week, mice were randomly allocated into groups fed an SC/NS (n = 24) or an HF-HS diet (n = 36). SC-NS and HF-HS diet were from GemPharmatech. SC-NS diet was composed of 10% fat, 0.4% salt, 66% carbohydrate, and 24% protein, presenting total calories of 3.22 kcal/g. HF-HS diet was composed of 60% fat, 8% salt, 20% carbohydrate, and 20% protein, presenting total calories of 5.24 kcal/g. After 4 weeks of dietary intervention, all mice were assigned to the following groups: (1) mice fed on an SC-NS diet; (2) mice fed on an SC-NS diet and TPPU supplement in drinking water; (3) mice fed on an HF-HS diet; (4) mice fed on an HF-HS diet and TPPU supplement in drinking water; and (5) mice fed on an HF-HS diet and dapagliflozin supplement in drinking water. Animals were randomized for the interventional subgroup (n = 12/group) and orally administered with TPPU (C<sub>16</sub>H<sub>20</sub>F<sub>3</sub>N<sub>3</sub>O<sub>3</sub>; Cayman Chemical) or dapagliflozin (Selleck) both at a dose of 1 mg/kg/day or vehicle for 8 consecutive weeks. Body weight, blood pressure, and blood glucose were monitored monthly. At the end of the study, mice were euthanized *via* cervical dislocation, and blood, urine, adipose, and kidneys were collected for further analysis.

All animal care and experimental procedures were reviewed and approved by the Experimental Animal Research Committee of Tongji Medical College, Huazhong University of Science and Technology (Wuhan, Hubei, China), and strictly complied with the Guide for the Care and Use of Laboratory Animals of the National Institutes of Health (Bethesda, MD).

### Blood pressure measurement

Blood pressure was measured by a noninvasive tail-cuff device (BP-2010A; Softron). The basal blood pressure of each group was recorded before the intervention and then monitored

monthly. The same person handled all measurements during a defined daytime period (between 2:00 and 5:00 PM). The tail-cuff approach was taken to determine arterial blood pressure and heart rate. To habituate the animals to the device and reduce variations in response to stress, there are several precautions including appropriate training of the mice over multiple days, prewarming tails to an appropriate temperature of 29 °C, measured in a quiet, semidark, and clean environment. After the measurement was stable, measured five times, and took the average to obtain a single representative value.

### Intraperitoneal glucose tolerance test and ITT determination

Intraperitoneal glucose tolerance tests were performed in all animals monthly. After determining basal blood glucose levels, glucose (2 g/kg body weight) was injected intraperitoneally into 16 to 17 h-fasted mice. Glucose levels from tail blood samples were monitored at 30, 60, 90, and 120 min by glucometer. ITTs were performed on 5-h-fasted mice injected intraperitoneally with 0.75 U/kg insulin. Blood glucose levels were determined as described previously.

### Metabolic parameter measurements

The metabolic analysis was performed by the Comprehensive Lab Animal Monitoring System with the Oxymax software (Columbus Instruments). Briefly, mice were individually caged in the metabolic chambers maintained at 20 to 22 °C in a 12-h light/12-h dark cycle, with an airflow of 0.6 l/min. After a 48-h acclimatization, VO<sub>2</sub>, VCO<sub>2</sub>, RER, food and water intake, and physical activity were simultaneously monitored every 10 min for 24 h. The value of VO<sub>2</sub> and VCO<sub>2</sub> was normalized to body weight (ml/kg/h). RER was calculated as VCO<sub>2</sub>/VO<sub>2</sub>, indicating the choice of metabolism substrate (fat or carbohydrate). Generally, an RER of 0.7 indicates pure fat oxidation, whereas an RER of 1.0 means pure carbohydrate oxidation, and a value between 0.7 and 1.0 suggests a mix of both fat and carbohydrate.

### WB

Kidney tissue or cell samples were ground and lysed in radioimmunoprecipitation assay buffer supplemented with protease inhibitors (separate cytoplasmic protein and nuclear protein according to the instructions). After measuring concentrations by the bicinchoninic acid method, protein samples were diluted to a concentration of 5 µg/µl and heated at 100 °C for 5 min with a denaturation buffer. Proteins were separated by 10% to 12% SDS-PAGE, transferred onto polyvinylidene difluoride membranes, and incubated overnight with primary antibodies at 4 °C. The membranes were washed with Tris-buffered saline with Tween 20 and incubated with HRP-conjugated goat anti-rabbit or antimouse secondary antibodies for 2 h at room temperature. Protein bands were visualized using enhanced chemiluminescent detection reagent. Finally, the ImageJ program (developed by the National Institutes of Health) was used to determine the density, which was normalized with β-actin or lamin B.

## TPPU alleviated insulin resistance and hypertension

### Cell culture and treatment

HK-2 cells were obtained from the Cell Bank of the Chinese Academy of Sciences and cultured in Dulbecco's modified Eagle's medium/F12, supplemented with 10% fetal bovine serum. Cells were cultured in a sterile incubator at 37 °C with a humidified atmosphere containing 5% CO<sub>2</sub>. When it came to 70% confluence, cells were incubated in a serum-free medium for 6 h. NaCl (20 nM) accompanied by palmitic acid (100 μM) was used to treat cells for 48 h. EETs (1, 10, 50 μM), TPPU (10 μM), dapagliflozin (10 μM), and BAY 11-7082 (30 μM) were used to pretreat cells after 6 h of starvation.

### siRNA transfection

The siEPHX2 and control siRNA were designed and synthesized by Ribobio. In brief, HK-2 cells were transfected with 50 nM of siRNA using Lipofectamine RNAiMAX (Invitrogen) when the confluence reached approximately 70%, and cell culture medium was changed 4 h later. Experiments were performed 48 h after transfection.

### Histology and IHC analysis

Adipose and kidney tissues were separated and immediately fixed with 4% paraformaldehyde for 24 h, then dehydrated, and embedded in paraffin. All tissues were sectioned with a thickness of 4 μm and stained with H&E. For immunohistochemistry, tissue sections were deparaffinized, rehydrated, antigen recovered in Tris-EDTA buffer (pH = 9.0), or sodium citrate buffer (pH = 6.0) through microwave for 20 min, washed in PBS. The sections were incubated with 3% H<sub>2</sub>O<sub>2</sub> in PBS for 30 min, followed by a 5% BSA solution for 1 h. Sections were then incubated with primary antibody overnight at 4 °C and followed with secondary antibodies for 2 h at room temperature. Then, sections were stained with hematoxylin after being developed with diaminobenzidine. Micrographs were acquired using light microscopy (OLYMPUS BX53). The quantification of staining was performed using ImagePro Plus software (Media Cybernetics).

### Immunofluorescence staining

After washed with PBS for three times, HK-2 cells were fixed with 4% paraformaldehyde and permeabilized using 0.2% Triton X-100 for 20 min. Cells were blocked with the appropriate serum and then incubated with primary antibodies overnight at 4 °C. The specimens were incubated with fluorescent secondary antibodies for 1 h in the dark. Nuclei were counterstained with 4',6-diamidino-2-phenylindole, and images were photographed under a fluorescence microscope (OLYMPUS BX53) with the same exposure time.

### Analysis of plasma and urine metabolites

Fasting and random blood glucose were measured from tail veins using a blood glucose meter (OneTouch Ultra) performed at baseline, and every 4 weeks, 24-h urine collection was carried out at the end of the experiment using metabolic cages. Urine levels of glucose and sodium were detected using

assay kits from Nanjing Jiancheng Bioengineering Institute according to the manufacturers' protocols. Kidney EET level was detected by 14,15-EET/dihydroxyeicosatrienoic acids ELISA kit following the manufacturer's instructions. Kidney sEH activity was detected by Soluble Epoxide Hydrolase Inhibitor Screening Assay Kit according to the manufacturers' instructions.

### Statistical analysis

Each experiment was repeated at least three times independently, and all data were expressed as mean ± SD. Statistical significance of differences among the groups was analyzed by Student's *t* test or one-way ANOVA for multiple comparisons followed by post hoc analyses to identify differences among groups. All the data were analyzed with SPSS 22.0 statistical software (SPSS, Inc). *p* < 0.05 was considered statistically significant.

### Data availability

All data are contained within the article and available from the corresponding author upon reasonable request.

**Acknowledgments**—We thank Dr Cong-Yi Wang and Dr Qing Zhou (Center for Biomedical Research of Tongji Hospital, Huazhong University of Science and Technology, China) for technical assistance with metabolic parameters analysis. We thank Dr Jiankun Yang (Experimental Medicine Research Center of Tongji Hospital, Huazhong University of Science and Technology, China) for technical assistance with histology.

**Author contributions**—X. X. and L. T. designed the research; J. L., S. H., M. F., W. L., L. L., Y. L., and Y. C. performed experiments; J. L., S. H., Y. Y., and R. D. analyzed data; J. L. and X. X. wrote the article. All authors approve the article. X. X. is the guarantor.

**Funding and additional information**—This work was supported by grants from the National Natural Science Foundation of China (no. 81873512 and no. 81471021).

**Conflict of interest**—The authors declare that they have no conflicts of interests with the contents of this article.

**Abbreviations**—The abbreviations used are: AUC, area under the curve; BSA, bovine serum albumin; DM, diabetes mellitus; EET, epoxyeicosatrienoic acid; ENaC, epithelial sodium channel; HF-HS, high-fat and high-salt; HK-2 cells, human renal proximal tubule epithelial cells; HRP, horseradish peroxidase; IHC, immunohistochemical; IKKα/β, inhibitory kappa B kinase α/β; ITT, insulin tolerance test; SC-NS, standard chow-normal salt; sEH, soluble epoxide hydrolase; SGLT2, sodium-glucose cotransporter 2; TPPU, trifluoromethoxyphenyl-3-(1-propionylpiperidin-4-yl) urea; VCO<sub>2</sub>, volume of carbon dioxide production; VO<sub>2</sub>, volume of oxygen consumption; RER, respiratory exchange ratio; WB, Western blot.

### References

1. Lastra, G., Syed, S., Kurukulasuriya, L. R., Manrique, C., and Sowers, J. R. (2014) Type 2 diabetes mellitus and hypertension: An update. *Endocrinol. Metab. Clin. North Am.* 43, 103–122

2. Muntner, P., Whelton, P. K., Woodward, M., and Carey, R. M. (2018) A comparison of the 2017 American College of Cardiology/American Heart Association blood pressure guideline and the 2017 American Diabetes Association Diabetes and Hypertension position statement for U.S. adults with diabetes. *Diabetes Care* **41**, 2322–2329
3. Ferrannini, E., and Cushman, W. C. (2012) Diabetes and hypertension: The bad companions. *Lancet* **380**, 601–610
4. DeFronzo, R. A., Ferrannini, E., Groop, L., Henry, R. R., Herman, W. H., Holst, J. J., Hu, F. B., Kahn, C. R., Raz, I., Shulman, G. I., Simonson, D. C., Testa, M. A., and Weiss, R. (2015) Type 2 diabetes mellitus. *Nat. Rev. Dis. primers* **1**, 15019
5. Kabakov, E., Norymberg, C., Osher, E., Koffler, M., Tordjman, K., Greenman, Y., and Stern, N. (2006) Prevalence of hypertension in type 2 diabetes mellitus: Impact of the tightening definition of high blood pressure and association with confounding risk factors. *J. Cardiometab. Syndr.* **1**, 95–101
6. Chen, G., McAlister, F. A., Walker, R. L., Hemmelgarn, B. R., and Campbell, N. R. C. (2011) Cardiovascular outcomes in Framingham participants with diabetes: The importance OF blood pressure. *Hypertension* **57**, 891–897
7. Wan, E. Y. F., Yu, E. Y. T., Chin, W. Y., Fung, C. S. C., Fong, D. Y. T., Choi, E. P. H., Chan, A. K. C., and Lo Lam, C. K. (2018) Effect of achieved systolic blood pressure on cardiovascular outcomes in patients with type 2 diabetes: A population-based retrospective cohort study. *Diabetes Care* **41**, 1134–1141
8. Eaddy, M. T., Shah, M., Lunacek, O., and Stanford, R. H. (2008) The burden of illness of hypertension and comorbid diabetes. *Curr. Med. Res. Opin.* **24**, 2501–2507
9. Adler, A. I., Stratton, I. M., Neil, H. A. W., Yudkin, J. S., Matthews, D. R., Cull, C. A., Wright, A. D., Turner, R. C., and Holman, R. R. (2000) Association of systolic blood pressure with macrovascular and microvascular complications of type 2 diabetes (UKPDS 36): Prospective observational study. *BMJ* **321**, 412–419
10. El-Sherbeni, A. A., and El-Kadi, A. O. S. (2014) The role of epoxide hydrolases in health and disease. *Arch. Toxicol.* **88**, 2013–2032
11. Merkel, M. J., Liu, L., Cao, Z., Packwood, W., Young, J., Alkayed, N. J., and van Winkle, D. M. (2010) Inhibition of soluble epoxide hydrolase preserves cardiomyocytes: Role of STAT3 signaling. *Am. J. Physiol. Heart Circ. Physiol.* **298**, H679–H687
12. Zhang, D., Xie, X., Chen, Y., Hammock, B. D., Kong, W., and Zhu, Y. (2012) Homocysteine upregulates soluble epoxide hydrolase in vascular endothelium *in vitro* and *in vivo*. *Circ. Res.* **110**, 808–817
13. Yang, H.-H., Duan, J.-X., Liu, S.-K., Xiong, J.-B., Guan, X.-X., Zhong, W.-J., Sun, C.-C., Zhang, C.-Y., Luo, X.-Q., Zhang, Y.-F., Chen, P., Hammock, B. D., Hwang, S. H., Jiang, J.-X., Zhou, Y., *et al.* (2020) A COX-2/sEH dual inhibitor PTUPB alleviates lipopolysaccharide-induced acute lung injury in mice by inhibiting NLRP3 inflammasome activation. *Theranostics* **10**, 4749–4761
14. Laethem, R. M., Balazy, M., Falck, J. R., Laethem, C. L., and Koop, D. R. (1993) Formation of 19(S)-, 19(R)-, and 18(R)-hydroxyecosatetraenoic acids by alcohol-inducible cytochrome P450 2E1. *J. Biol. Chem.* **268**, 12912–12918
15. Shen, H. C. (2010) Soluble epoxide hydrolase inhibitors: A patent review. *Expert Opin. Ther. Patents* **20**, 941–956
16. Wright, E. M., and Turk, E. (2004) The sodium/glucose cotransport family SLC5. *Pflugers Arch.* **447**, 510–518
17. Zelniker, T. A., and Braunwald, E. (2018) Cardiac and renal effects of sodium-glucose Co-transporter 2 inhibitors in diabetes: JACC state-of-the-art review. *J. Am. Coll. Cardiol.* **72**, 1845–1855
18. Hummel, C. S., Lu, C., Loo, D. D. F., Hirayama, B. A., Voss, A. A., and Wright, E. M. (2010) Glucose transport by human renal Na<sup>+</sup>/d-glucose cotransporters SGLT1 and SGLT2. *Am. J. Physiol. Cell Physiol.* **300**, C14–21
19. Rahmoune, H., Thompson, P. W., Ward, J. M., Smith, C. D., Hong, G., and Brown, J. (2005) Glucose transporters in human renal proximal tubular cells isolated from the urine of patients with non-insulin-dependent diabetes. *Diabetes* **54**, 3427–3434
20. Heerspink, H. J. L., Perkins, B. A., Fitchett, D. H., Husain, M., and Cherney, D. Z. I. (2016) Sodium glucose cotransporter 2 inhibitors in the treatment of diabetes mellitus: Cardiovascular and kidney effects, potential mechanisms, and clinical applications. *Circulation* **134**, 752–772
21. Fu, M., Yu, J., Chen, Z., Tang, Y., Dong, R., Yang, Y., Luo, J., Hu, S., Tu, L., and Xu, X. (2021) Epoxyecosatrienoic acids improve glucose homeostasis by preventing NF-κB-mediated transcription of SGLT2 in renal tubular epithelial cells. *Mol. Cell Endocrinol.* **523**, 111149
22. Xu, X., Zhao, C. X., Wang, L., Tu, L., Fang, X., Zheng, C., Edin, M. L., Zeldin, D. C., and Wang, D. W. (2010) Increased CYP2J3 expression reduces insulin resistance in fructose-treated rats and db/db mice. *Diabetes* **59**, 997–1005
23. Yang, Y., Dong, R., Chen, Z., Hu, D., Fu, M., Tang, Y., Wang, D. W., Xu, X., and Tu, L. (2018) Endothelium-specific CYP2J2 overexpression attenuates age-related insulin resistance. *Aging Cell* **17**, e12718
24. Makita, K., Takahashi, K., Karara, A., Jacobson, H. R., Falck, J. R., and Capdevila, J. H. (1994) Experimental and/or genetically controlled alterations of the renal microsomal cytochrome P450 epoxygenase induce hypertension in rats fed a high salt diet. *J. Clin. Invest.* **94**, 2414–2420
25. Capdevila, J. H., Pidkova, N., Mei, S., Gong, Y., Falck, J. R., Imig, J. D., Harris, R. C., and Wang, W. (2014) The Cyp2c44 epoxygenase regulates epithelial sodium channel activity and the blood pressure responses to increased dietary salt. *J. Biol. Chem.* **289**, 4377–4386
26. Imig, J. D., Zhao, X., Zaharis, C. Z., Olearczyk, J. J., Pollock, D. M., Newman, J. W., Kim, I.-H., Watanabe, T., and Hammock, B. D. (2005) An orally active epoxide hydrolase inhibitor lowers blood pressure and provides renal protection in salt-sensitive hypertension. *Hypertension* **46**, 975–981
27. Jiang, H., Anderson, G. D., and McGiff, J. C. (2011) The red blood cell participates in regulation of the circulation by producing and releasing epoxyecosatrienoic acids. *Prostaglandins Other Lipid Mediat.* **98**, 91–93
28. Zhang, L.-N., Vincelette, J., Chen, D., Gless, R. D., Anandan, S.-K., Rubanyi, G. M., Webb, H. K., MacIntyre, D. E., and Wang, Y.-X. J. (2011) Inhibition of soluble epoxide hydrolase attenuates endothelial dysfunction in animal models of diabetes, obesity and hypertension. *Eur. J. Pharmacol.* **654**, 68–74
29. Zuloaga, K. L., Krasnow, S. M., Zhu, X., Zhang, W., Jouihan, S. A., Shangraw, R. E., Alkayed, N. J., and Marks, D. L. (2014) Mechanism of protection by soluble epoxide hydrolase inhibition in type 2 diabetic stroke. *PLoS One* **9**, e97529
30. Sabolic, I., Vrhovac, I., Erer, D. B., Gerasimova, M., Rose, M., Breljak, D., Ljubojevic, M., Brzica, H., Sebastiani, A., Thal, S. C., Sauvart, C., Kipp, H., Vallon, V., and Koepsell, H. (2012) Expression of Na<sup>+</sup>-D-glucose cotransporter SGLT2 in rodents is kidney-specific and exhibits sex and species differences. *Am. J. Physiol. Cell Physiol.* **302**, C1174–C1188
31. Koepsell, H. (2017) The Na<sup>+</sup>-D-glucose cotransporters SGLT1 and SGLT2 are targets for the treatment of diabetes and cancer. *Pharmacol. Ther.* **170**, 148–165
32. Vallon, V. (2015) The mechanisms and therapeutic potential of SGLT2 inhibitors in diabetes mellitus. *Annu. Rev. Med.* **66**, 255–270
33. Vallon, V., and Thomson, S. C. (2012) Renal function in diabetic disease models: The tubular system in the pathophysiology of the diabetic kidney. *Annu. Rev. Physiol.* **74**, 351–375
34. Pidkova, N., Rao, R., Mei, S., Gong, Y., Harris, R. C., Wang, W.-H., and Capdevila, J. H. (2013) Epoxyecosatrienoic acids (EETs) regulate epithelial sodium channel activity by extracellular signal-regulated kinase 1/2 (ERK1/2)-mediated phosphorylation. *J. Biol. Chem.* **288**, 5223–5231
35. Wei, Y., Lin, D.-H., Kemp, R., Yaddanapudi, G. S. S., Nasjletti, A., Falck, J. R., and Wang, W.-H. (2004) Arachidonic acid inhibits epithelial Na channel via cytochrome P450 (CYP) epoxygenase-dependent metabolic pathways. *J. Gen. Physiol.* **124**, 719–727
36. Pavlov, T. S., Ilatovskaya, D. V., Levchenko, V., Mattson, D. L., Roman, R. J., and Staruschenko, A. (2011) Effects of cytochrome P-450 metabolites of arachidonic acid on the epithelial sodium channel (ENaC). *Am. J. Physiol. Ren. Physiol.* **301**, F672–F681
37. Shoelson, S. E., Lee, J., and Goldfine, A. B. (2006) Inflammation and insulin resistance. *J. Clin. Invest.* **116**, 1793–1801
38. Lu, X., and Crowley, S. D. (2018) Inflammation in salt-sensitive hypertension and renal damage. *Curr. Hypertens. Rep.* **20**, 103

## TPPU alleviated insulin resistance and hypertension

39. Olefsky, J. M., and Glass, C. K. (2010) Macrophages, inflammation, and insulin resistance. *Annu. Rev. Physiol.* **72**, 219–246
40. Imig, J. D., Jankiewicz, W. K., and Khan, A. H. (2020) Epoxy fatty acids: From salt regulation to kidney and cardiovascular therapeutics: 2019 Lewis K. Dahl memorial lecture. *Hypertension* **76**, 3–15
41. Guzik, T. J., and Cosentino, F. (2018) Epigenetics and immunometabolism in diabetes and aging. *Antioxid. Redox Signal.* **29**, 257–274
42. Hye Khan, M. A., Neckár, J., Manthali, V., Errabelli, R., Pavlov, T. S., Staruschenko, A., Falck, J. R., and Imig, J. D. (2013) Orally active epoxyeicosatrienoic acid analog attenuates kidney injury in hypertensive Dahl salt-sensitive rat. *Hypertension* **62**, 905–913
43. Li, R., Xu, X., Chen, C., Wang, Y., Gruzdev, A., Zeldin, D. C., and Wang, D. W. (2015) CYP2J2 attenuates metabolic dysfunction in diabetic mice by reducing hepatic inflammation via the PPAR $\gamma$ . *Am. J. Physiol. Endocrinol. Metab.* **308**, E270–E282
44. Olearczyk, J. J., Quigley, J. E., Mitchell, B. C., Yamamoto, T., Kim, I.-H., Newman, J. W., Luria, A., Hammock, B. D., and Imig, J. D. (2009) Administration of a substituted adamantyl urea inhibitor of soluble epoxide hydrolase protects the kidney from damage in hypertensive Goto-Kakizaki rats. *Clin. Sci. (Lond.)* **116**, 61–70
45. Baker, R. G., Hayden, M. S., and Ghosh, S. (2011) NF- $\kappa$ B, inflammation and metabolic disease. *Cell Metab.* **13**, 11–22
46. Tornatore, L., Thotakura, A. K., Bennett, J., Moretti, M., and Franzoso, G. (2012) The nuclear factor kappa B signaling pathway: Integrating metabolism with inflammation. *Trends Cell Biol.* **22**, 557–566
47. Han, H. J., Oh, Y. J., and Lee, Y. J. (2005) Effect of albumin on <sup>14</sup>C-alpha-Methyl-D-Glucopyranoside uptake in primary cultured renal proximal tubule cells: Involvement of PLC, MAPK, and NF-kappaB. *J. Cell. Physiol.* **202**, 246–254
48. Lee, Y. J., Heo, J. S., Suh, H. N., Lee, M. Y., and Han, H. J. (2007) Interleukin-6 stimulates alpha-MG uptake in renal proximal tubule cells: Involvement of STAT3, PI3K/Akt, MAPKs, and NF-kappaB. *Am. J. Physiol. Ren. Physiol.* **293**, F1036–F1046